Cracking on Embankment Dams due to Recent Large Earthquakes and Direct and Splitting Tensile Strength Tests for Core Material

H. SATO & Y. ENOMURA
Public Works Research Institute (PWRI), Tsukuba, Japan
h-sato@pwri.go.jp

Y. YAMAGUCHI
Japan Dam Engineering Center (JDEC), Tokyo, Japan

ABSTRACT

The 2011 Tohoku Earthquake and other large earthquakes in recent years in Japan have caused relatively large cracks on the crests of some embankment dams. Immediately after the 2011 Tohoku Earthquake, special safety inspections were carried out at over 300 dams in the affected area. As a result of these inspections, more than 10% of all inspected dams reported some damages. This ratio rose to 18% for embankment dams. Damage to embankment dams included relatively wide and/or long cracks mainly on the crests of earthfill dams. After the 1995 Kobe Earthquake, cracks were also observed on the crest of the Kinjoike dam, an old earthfill dam with a height of 15m located about 30km from the epicenter. The width of the crack on the crest was narrow about 1cm, but the crack extended deep into the dam when the dam was excavated to perform repairing work while checking the crack extension. However, no sliding deformation was observed at the Kinjoike dam. Results of safety inspections of embankment dams after large earthquakes in Japan have raised awareness of the importance of evaluating cracks of embankment dams. It is necessary to evaluate tensile strengths of materials of embankment dams, but almost no tensile strength tests using materials of embankment dams have been carried out. In this paper, we firstly introduce cracking generated on embankment dams due to recent large earthquakes. Next, we report the results of laboratory direct and splitting tensile tests using core material of an existing rockfill dam.

Keywords: Embankment Dam, Earthquake, Cracking, Tensile Strength.

1. INTRODUCTION

When designing embankment dams, levees, and other structures made of soil or other geotechnical materials, the tensile strength of the materials is normally ignored. It is ignored, presumably because the tensile strength of geotechnical material is much lower than its compressive strength and it is not easy to measure the tensile strength of geotechnical materials. But, it is believed that one cause of phenomena such as slope failure or hydraulic fracturing of geotechnical materials during construction of levees etc. and/or during excavation of a slope is cracking caused by tension, and it is important to evaluate the tensile strength of geotechnical materials in order to evaluate the occurrence and progress of cracking.

Results of the safety inspections of embankment dams after the large earthquakes have raised awareness of the importance of evaluating crack extension of embankment dam body crests and local failure of the boundaries of embankment dam bodies and concrete structures. It is necessary to evaluate the tensile strength of dam body material of embankment dams. But almost no tensile strength tests using construction materials of embankment dams have been carried out. In this research, core material of an existing rockfill dam was used to perform direct and splitting tensile tests, to study the impact of degree of compaction and other test conditions on tensile strength.

2. CRACKING ON EMBANKMENT DAM BODIES DUE TO RECENT LARGE EARTHQUAKES IN JAPAN

Japan is one of the most prone countries to large earthquakes. Based on the results of post-earthquake investigations on embankment dams and "Tame-ike", small agricultural pond, in Japan, there are three typical damage types of embankment dams due to recent large earthquakes shown in Figure 1. In this paper, we focus on the third damage type of cracks on the crest without sliding in Figure 1. Some technical papers of cracking on embankment dams have been reported after some large earthquakes in Japan.

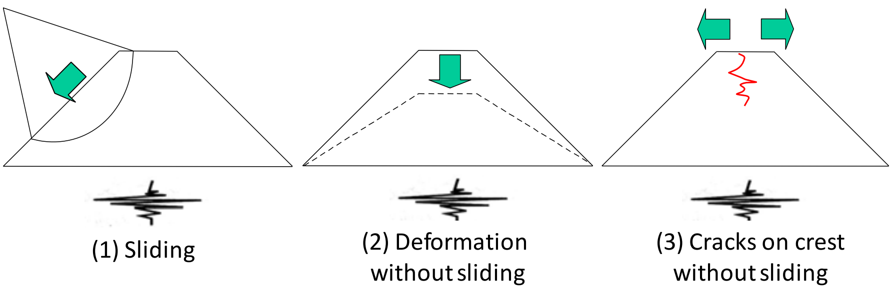

Figure 1. Typical damage types of embankment dams due to recent large earthquakes

In 1923, because the Great Kanto earthquake hit around Tokyo area, some earthfill dams including the Oono dam and the Murayama upper and lower dams were cracked on the dam body crests. (Okamoto, 1985)

In 1964, after the Niigata earthquake hit around Niigata city, safety inspections for agricultural earthfill dams were conducted and the number of damaged earthfill dams was 146 among about 8700 inspected earthfill dams. No earthfill dams were failed during the earthquake, but 7 earthfill dams were collapsed after some days later than the earthquake day because of such as late seepage failure through cracks in the dam body due to the earthquake. Cracking on the crests and upstream surfaces of earthfill dams was the main damage due to the earthquake and cracking were observed in about 80 % of the 146 damaged earthfill dams. (Takase, 1966)

Figure 2 is a photo of the Kinjoike dam, an agricultural old eathfill dam where the crest of the dam was cracked by the Kobe earthquake in 1995. The Kinjoike dam is an earthfill dam with a central core about 15 m high and 176 m long located about 30 km from the epicenter. The construction year of the Kinjoike dam has been unknown, but it was redeveloped around 1960. It was confirmed that the Kobe earthquake in 1995 generated a 75m long crack in the center of the crest of the Kinjoike dam. As shown in Figure 2, the width of the crack on the crest was small at about 1cm. However, when the dam body was excavated to perform repairing works while checking the depth of the cracks, it was confirmed that cracking from the crest extended deep into the dam body as shown in the left side of Figure 3 (Hyogo Prefecture, 1996). The right side of Figure 3 shows the location of the Kinjyoike dam.

Figure 2. Crack on the crest (left) and repairing work (right) of the Kinjoike dam after the Kobe earthquake in 1995 (Hyogo Prefecture, 1996)

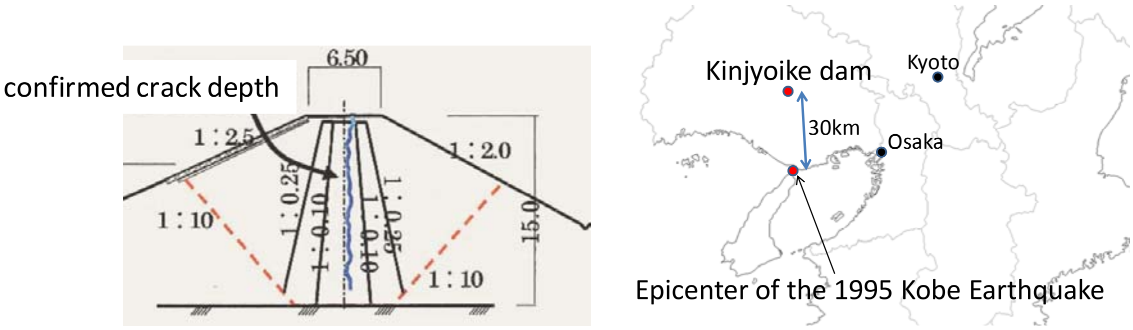

Figure 3. Crack depth of the Kinjoike dam after the Kobe earthquake in 1995 (left) and location of the Kinjyoike dam (Hyogo Prefecture, 1996)

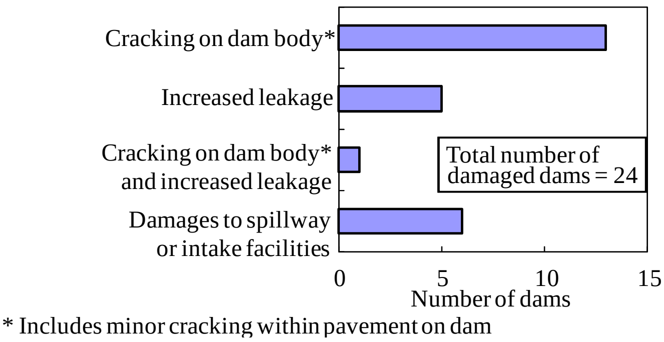

Figure 4. Damage types of embankment dams after the Tohoku earthquake in 2011 (Yamaguchi et al., 2012)

The Tohoku earthquake in 2011 and other large earthquakes which have occurred in recent years in Japan have caused relatively large cracks on the crests of many embankment dams. Immediately after the 2011 Tohoku Earthquake, special safety inspections were carried out at over 300 dams in the affected area. As a result of special safety inspections, more than

10% of all inspected dams reported some damages. This ratio rose to 18% for embankment dams. Damage of embankment dams included relatively wide and/or long cracks mainly on the crests of earthfill dams. 133 embankment dams were inspected, and 24 embankment dams were reported some minor damages, mainly cracking on dam body shown in Figure 4. At several dams, reservoir drawdown was necessary to ensure safety and enable investigations to identify the area and cause of the damage. (Yamaguchi et al., 2012)

3. FUNDAMENTAL PHYSICAL PROPERTIES OF CORE MATERIAL FOR TENSILE STRENGTH TESTS

3.1. Test Material

Test material was core material of an existing rockfill dam with a center core. The core material was a mixed material including coarse and fine grain material. The coarse-grain material was obtained from alternating layers of mudstone, sandstone, and lapilli tuff, while the fine grain material was talus and deposited sediment. The material was prepared by mixing at the on-site stockpile, then maximum grain size was adjusted to 2 mm. Figure 5 shows the grain size distribution of the test material.

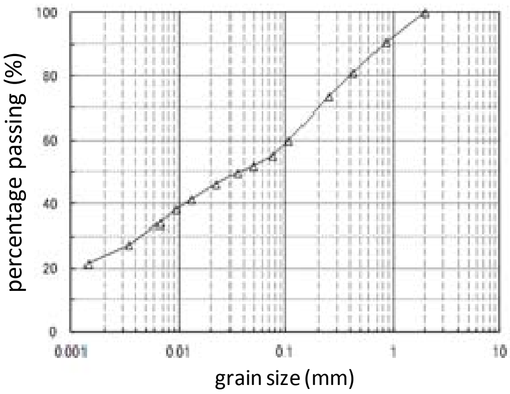

Figure 5. Grain size distribution of test material

Table 1. Results of unconfined compression tests

degree of compaction	specimen	unconfined compression strength
(%)	No.	q_u(kN/m^2)
95	1	281.9
	2	282.6
	3	278.2
	average	280.9
100	1	372.4
	2	361.8
	3	381.8
	average	372.0

3.2. Unconfined Compression Tests for Core Material

The unconfined compression tests were conducted according to the Unconfined Compression Test Method of Soil (JIS A1216). The columnar specimens were height of

100 mm and diameter of 50 mm. The degree of compaction was set for 2 cases of 95 % and 100 % and they were prepared at the optimum water content. Specimens were compacted devided in five layers. The strain ratio of the unconfined compression tests was set at 1 % per minute. Three specimens were tested for each case. Table 1 shows the results of the unconfined compression tests.

The result show that the higher the degree of compaction, the higher the unconfined compressive strength.

4. SPLITTING TENSILE STRENGTH TESTS FOR CORE MATERIAL

4.1. Test Method

The splitting tensile strength tests were conducted according to Concrete Splitting Tensile Strength Test Method (JIS A1113). The splitting tensile strength is calculated according to Eq. 1, theoretically.

$$f_t = \frac{2P}{\pi dl} \qquad (1)$$

Where, f_t: splitting tensile strength, P: maximum compressive load, d: diameter of the specimen, and l: length of the specimen. The dimensions of the specimens were both diameter and height of 50 mm. The specimens were compacted by five compaction layers. To study the effects of the degree of compaction and the loading velocity, the splitting tensile strength tests were conducted for the test cases shown in Table 2. Three specimens were tested for each case in Table 2. Regarding the compression ratio, the maximum and the minimum compression ratios of the test equipment were 5 mm/min and 0.05 mm/min respectively, and a medium value of 0.5 mm/min was also set.

Figure 6 shows a photo of the test. To measure displacements in the tensile direction, as shown in Figure 6, pushpins were placed at the sides of the specimens, and displacement gauges were attached to them to measure the displacements in the orthogonal direction to the compression direction.

4.2. Test Results

Figures 7 and 8 show the specimens after the tests. Although the specimens after the tests are, as shown in the photos, considered to be slightly affected by the loading plate, cracks formed vertically in almost the center of the specimens in every case.

Table 3 shows the results of the splitting tensile strength tests. Like the results of the unconfined compression tests, variations of the splitting tensile strengths were small among the three specimens in each case.

5. DIRECT TENSILE STRENGTH TESTS FOR CORE MATERIAL

5.1. Test Method

The test device was developed by Tamrakar (Tamrakar, 2004) shown in Figures 9. The test

Table 2. Cases for the splitting tensile tests

maximum grain size (mm)	degree of compaction (%)	water content (%)	compression ratio (mm/min)	number of tests
2	95	w_{opt}	0.5	3
2	100	w_{opt}	0.05	3
2	100	w_{opt}	0.5	3
2	100	w_{opt}	5	3

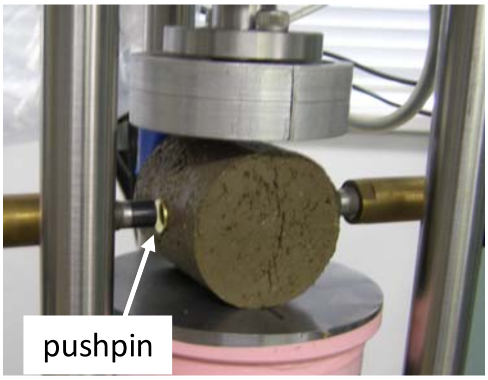

Figure 6. Photo of the splitting tensile test

Figure 7. Specimens after the splitting tensile tests (D=95%)

Figure 8. Specimens after the splitting tensile tests (D=100%)

Table 3. Results of the splitting tensile tests

degree of compaction D(%)	dry density ρ_d (g/cm^3)	compression ratio (mm/min)	displacement orthogonally to loading direction at maximum compression stress (mm)				splitting tensile strength (kPa)			
			No1	No2	No3	average	No1	No2	No3	average
95	1.413	0.5	0.458	0.396	0.634	0.496	22.7	23.3	22.4	22.8
100	1.487	0.5	0.260	0.152	0.248	0.220	24.4	26.0	26.2	25.5
100	1.487	0.05	0.224	0.194	0.346	0.255	22.7	22.9	21.8	22.5
100	1.487	5	0.210	0.334	0.194	0.246	30.7	27.5	30.4	29.5

device is made up of two parts, a fixed part and a movable part. The movable part can move freely in the tensile direction using a linear slide under the movable part. The frictional resistance during slide is almost zero because of the linear slide under the movable part. The surface area of the mold is 38.5 cm^2, its depth is 5cm and the width of the contact part of the mold is 3 cm as shown in the right side of Figure 9. The tensile force is measured by a load cell on the movable side in Figure 9.

The test material was adjusted to the optimum water content, then placing the material necessary for the target degree of compaction inside the mold, placing a collar on the top of the mold, and statically pressing the collar from above with a loading plate of the same shape as the mold cross section to compact the specimen. The mold with depth of 5 cm was compacted divided into four layers.

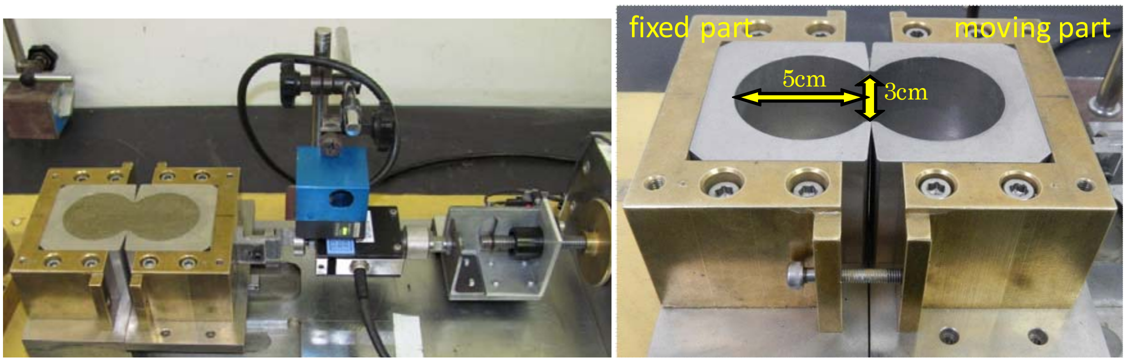

Figure 9. The direct tensile test equipment (left) and the test mold (right)

5.2. Test Conditions

The test conditions were set at two degrees of compaction: 95 % and 100 %. The tensile strain ratio was set at three values: 0.01 mm/min, 0.1 mm/min, and 1 mm/min. Three specimens were tested under each test case of a total of 6 sets of test conditions set combining 2 degrees of compaction and 3 tensile strain ratios.

5.3. Test Results

Figure 10 shows the specimens for the direct tensile strength tests before and after the tests. On the specimens after the tests, the crack that formed at the time of failure was straight line in the center of the specimens in every test case.

Figure 11 shows the relationship of displacement and tensile stress at the degrees of compaction of 95 % and 100 %. Tensile stresses show clear peaks, and when displacements were higher than about 1 mm, tensile stresses were almost zero.

Figure 12 shows the relationship of tensile strain ratio and tensile strength. The tensile strength at the degree of compaction 100% is about 10 kPa larger than the tensile strength of the degree of compaction of 95 %. The larger the tensile strain ratio, the larger the tensile strength tends.

Figure 13 shows the relationship of displacement at the failure and tensile strength. The displacement at the failure means the displacement value when the tensile stress has peak value in Figure 11. Figure 13 shows the result for each degree of compaction and for each tensile strain ratio. The displacement at the time of failure was distributed roughly from 0.05 mm to 0.1 mm. The displacements at the time of failure at the degree of compaction of 100 % tend to be slightly larger than those of 95 %, but it is not very clear.

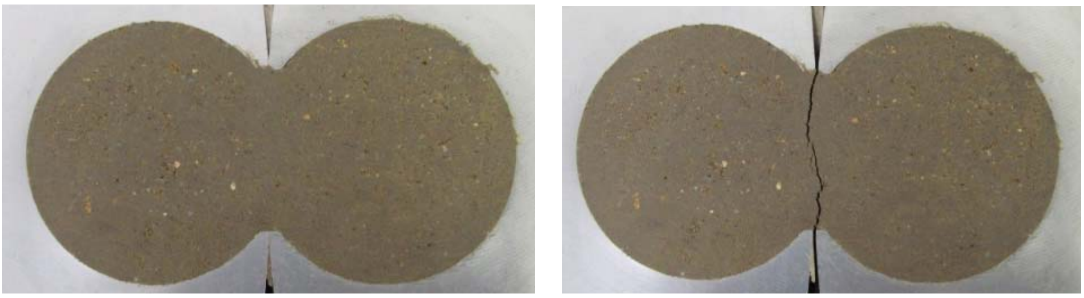

Figure 10. Specimen before (left) and after (right) the direct tensile test

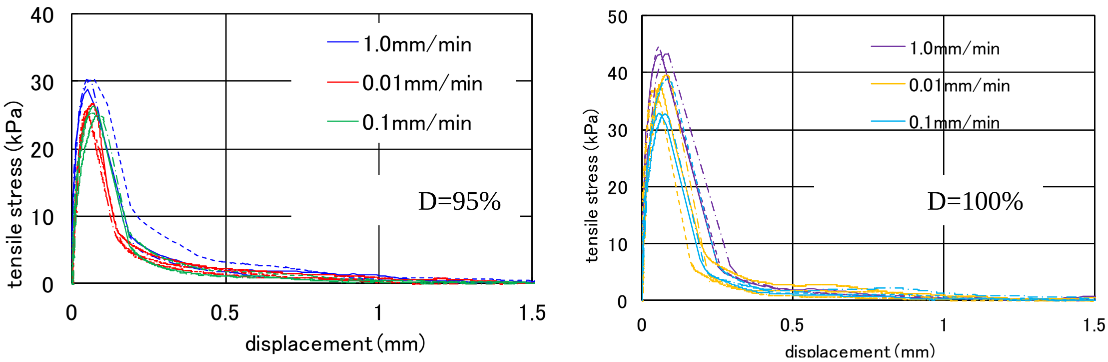

Figure 11. Relationships between displacement and tensile stress

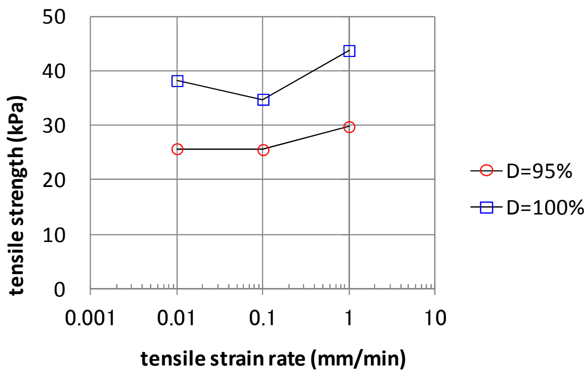

Figure 12. Relationships between tensile strain ratio and tensile strength

Figure 14 shows both the splitting tensile strengths and the direct tensile strengths. Figure 14 categorizes the tensile strain ratio based on degree of compaction as the horizontal axis and shows the direst and splitting tensile strengths. Figure 14 shows that the direct tensile strengths tend to be higher than the splitting tensile strengths, and that the direct tensile strengths at the degree of compaction of 100% in particular, are larger from 10 to 20 kPa than the splitting tensile strengths. Like the direct tensile strength, the splitting tensile strength increases as the tensile strain ratio rises.

Table 4 shows the results of the direct tensile strength tests and the unconfined compressive strength tests. When the degree of compaction is 95 %, the ratio of the direct tensile strength to the unconfined compressive strength ranges from 9.1 % to 10.6 %. When the degree of compaction is 100 %, the ratio of the direct tensile strength to the unconfined compressive strength ranges from 9.4 % to 11.8 %. As the ratio of the direct tensile strength to the unconfined compressive strength is within the range of values in the tensile strength test results based on existing core materials or soil materials (Sato, 2008). Because the ratio is similar to that of concrete, tensile strength of soil material and other core materials of rockfill dams may be able to be estimated with a certain degree of precision based on unconfined compressive strength.

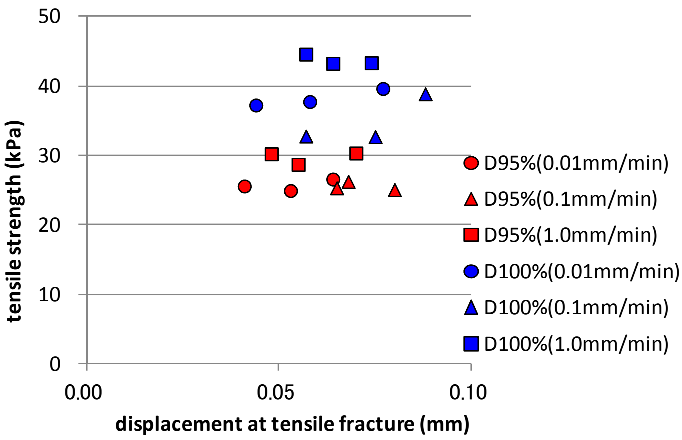

Figure 13. Relationships between displacement at failure and tensile strength

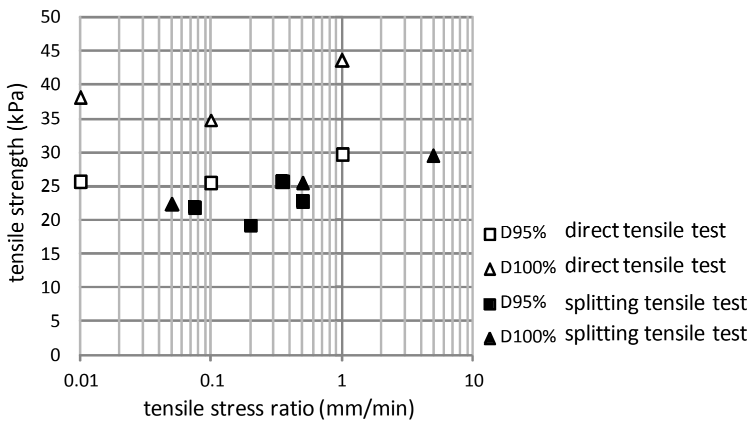

Figure 14. Comparison of results of splitting and direct tensile tests

Table 4. Relationship between direct tensile strength and unconfined compressive strength

degree of compaction	tensile strain ratio (mm/min)	direct tensile strength (kPa)	unconfined compressive strength (kPa)	direct tensile strength/unconfined compressive strength
95%	0.01	25.72	280.9	0.092
	0.1	25.56		0.091
	1	29.77		0.106
100%	0.01	38.21	372.0	0.103
	0.1	34.78		0.093
	1	43.72		0.118

6. CONCLUSIONS

In this paper, we focus on cracking on embankment dams due to large earthquakes. We introduce some examples of cracking on embankment dams due to large earthquakes in Japan. Because tensile properties of embankment materials are important, the splitting and direct tensile tests were conducted using core material of an existing rockfill dam. During the tests, straight tension cracks at the center of the specimens were observed. Based on the results of the splitting and direct tensile tests, the tensile strength of the specimen with the higher degree of compaction tended to be larger. And if the tensile strain ratio was larger, the tensile strength also tended to be larger. These tests revealed that the ratio of the direct tensile strength to the unconfined compressive strength is about 0.1, which is within the range of the results of the existing tensile tests of soil materials.

As Sherard pointed out in his paper (Sherard, 1973), the tensile strengths of the core material have some relationships to the degree of compactions. Tatsuoka also pointed out in his paper (Tatsuoka, 2006) that the better the degree of compaction of embankment dams, the better the performance of embankment dams against sliding deformation, settlement and cracking due to earthquakes. The results in this paper agree with these opinions of the specialists.

In the future, we wish to conduct research to evaluate tensile strength of core materials using other embankment dams and to clarify the mechanism of cracking and evaluate the crack depth on the crest of embankment dams during earthquakes. We also wish to conduct analysis which can reproduce cracks due to earthquakes and develop a method to evaluate safety of embankment dams during large earthquakes based on the results of crack analysis.

REFERENCES

S. Okamoto (1985): *Design of Structures considering Seismic Forces*, 226p., Japan (in Japanese).

K. Takase (1966): *Damage to Earthfill Dams due to Earthquakes*, Soil mechanics and foundation engineering, the Japanese Geotechnical Society, Vol.14, No.10, pp.3-9, Japan (in Japanese).

Hyogo Prefecture (1996): *Records of Damages to Agricultural Facilities during the Kobe Earthquake*, Japan (in Japanese).

Y. Yamaguchi, M. Kondo and T. Kobori (2012): *Safety Inspections and Seismic Behavior of Embankment Dams during the 2011 off the Pacific Coast of Tohoku Earthquake*, Soils and Foundation, the Japanese Geotechnical Society, Vol.52, Issue5, pp.945-955, Japan.

S. B. Tamrakar, Y, Toyosawa and K. Itoh (2004): *Tensile Strength of Compacted and Saturated Soils using Newly Developed Tensile Strength Measuring Apparatus*, 39th Japan National Conference of Geotechnical Engineering, pp.251-252, Japan.

H. Sato and Y. Yamaguchi (2008): *Effect of Consolidation on Split Tensile Strength of Core Materials after Cracking*, Engineering for dams, Japan Dam Engineering Center, vol.262, pp.28-35, Japan (in Japanese).

Sherard, J. L. (1973): *Embankment dam cracking*, Embankment Dam Engineering, pp.271-353, New York.

F. Tatsuoka (2006): *Visions for Seismic Design of Rockfill Dams*, Engineering for Dams, Japan Dam Engineering Center, No.243, pp.1-2, Japan (in Japanese).